EMERGING TECH CONFERENCE – Edge Intelligence

Volume 02, 2023, Page 131 – 137

Proceedings of Emerging Tech Conference:
Edge Intelligence 2023

Fault Detection in Analog Circuits by utilizing the Current Supply Transients

Vassilios D. Vassios[1] ,Argirios.T.Hatzopoulos[1] , Ioannis G. Intzes[1] and Dimitrios K. Papakostas[1]
[1]*Department of Information and Electronic Engineering International*
Hellenic University Thessaloniki, Greece
vassios@yahoo.com, ahatz@ihu.gr, intzes@iee.ihu.gr, dpapakos@ihu.gr

Abstract

An improved method in fault detection in Analog Circuits is presented in this paper. The CUTs are subjected to a short undervoltage, and the transient current is measured. From the current measurement of the power supply during this time the mean and fundamental rms values are calculated. From these measurements for both the mean and the fundamental values three points of interest are extracted. The maximum/minimum over/undershooting values, the relaxation point values, and the damping point values. These twelve points of interest comprise the signature for comparison for all the subsequent CUTs. The algorithm is tested both in simulation and with actual measurements with actual CUTs.

1 Introduction

Fault detection in analog and mixed signal circuits is a continuous field of research and development. A vast variety of techniques and algorithms have been proposed over the years. Fault detection is a practice the IC manufacturers and electronic devices industries use to achieve higher quality and reliability for their customers. Also, these techniques help to improve the repair times of machines that use these electronic devices[1].

Numerous methodologies and algorithms are proposed for fault identification, which include fault dictionary methods [2], IPS measurement [3], the rms approach[4] and many others. Several different signatures can be created by using several metrics, including magnitude/phase [5], spectral analysis [6], wavelet decomposition [7], and a multitude of mathematical techniques such as statistical analysis (standard deviation) [8], topological analysis (Malahanobis distance) [9]. For this paper, the Under/Over Voltage (UOV) algorithm is presented. In this algorithm the IPS is measured, and the moving average/fundamental rms algorithms are used to produce the signature fields and calculate the region of interest in the waveforms without performing any complex or time-consuming calculations.

2 Review of the Algorithm

Analog and mixed signal circuits continue to function properly even if they experience a small fluctuation in their power supply line. The Under/Over Voltage algorithm relies on this property. The proposed algorithm processes the power supply's Current and calculates the overshooting, undershooting and damping values of the supply current's waveforms in respect to the time they occurred.

The algorithm consists of several steps, which are analyzed in more detail in the paragraph below.

Step 1) Wait for the CUT to stabilize in its normal operating mode.

Step 2) The CUT suffers a small under-voltage in its power supply line (Negative Step).

Step 3) The power supply current to the CUT is measured and the mean, true rms and fundamental rms values are calculated.

Step 4) The maximum/minimum value for the current over/undershooting and the damping point for both the Mean and fundamental rms are calculated along with the time they occurred.

Step 5) The CUT is driven back to its normal voltage supply values (Positive Step).

Step 6) Steps 3 and 4 are repeated one more time for the Positive Step and all the corresponding current and time value pairs are calculated.

Step 7) The twelve different current value/time pairs, six the mean values and six for fundamental rms values, comprise the signature library.

Step 8) Using Monte Carlo simulation, steps 1 through 7 are repeated to calculate the variance σ and generate a detection area of the typical current/time values that can be compared to all other measurements.

The measurements on actual CUTs in Step 8 are substituted for the Monte Carlo simulations by the actual experimental data.

3 Implementation of the Algorithm

A small and simple CE amplifier, as shown in Fig.1. The circuit's behavior operation was first simulated with the PSpice module from Altium Designer 20 and then the actual circuit was designed and constructed for verification or disproval of the simulation results. The circuit is stimulated with a sinusoidal signal that has a 1kHz frequency and an amplitude of 10mV(p-p) to drive it. In the experimental setting the supply current is measured with the use of a current sense amplifier by measuring the differential voltage drop along a shunt resistor[11]. Additionally, a digital to analog converter is used to generate the sinusoidal signal from a microcontroller. Step 2 changes the circuit's power consumption state, or the I_{PS}, by reducing the supply voltage by 10% from its nominal value. These actions are depicted in Fig. 2. The waveforms are separated into two sections. The transition from 100% to 90% of the power-supply voltage constitutes the first section and will be referred as the Negative Step (NS), and the transition from 90% to 100% of the power-supply voltage constitutes the second section and will be referred as the Positivity Step (PS). The time duration for both steps is defined as the time between transitions and is extracted from trial-and-error simulations. The same algorithm was used to process the two sections separately.

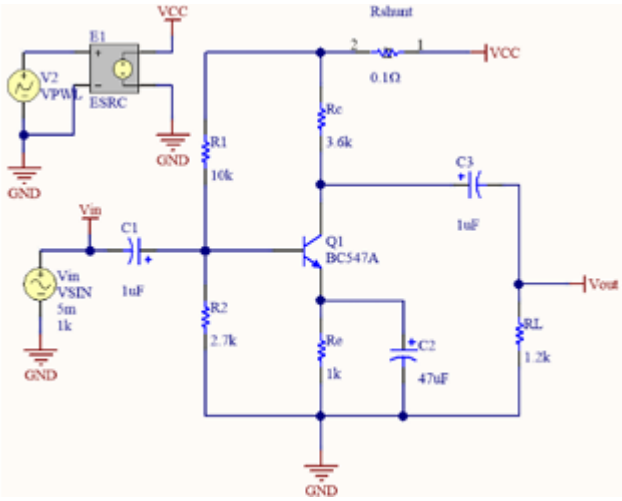

Figure 1. Schematic Description of the CE amplifier

From the author's previous work [22], it became apparent that the mean and the true rms calculations have very close values which forces the algorithm to be unable to recognize a significant number of Faults. In that scope, the "fundamental rms" is used in the current work. These similarities and differences between the mean, true rms and fundamental rms are shown in Fig.3.

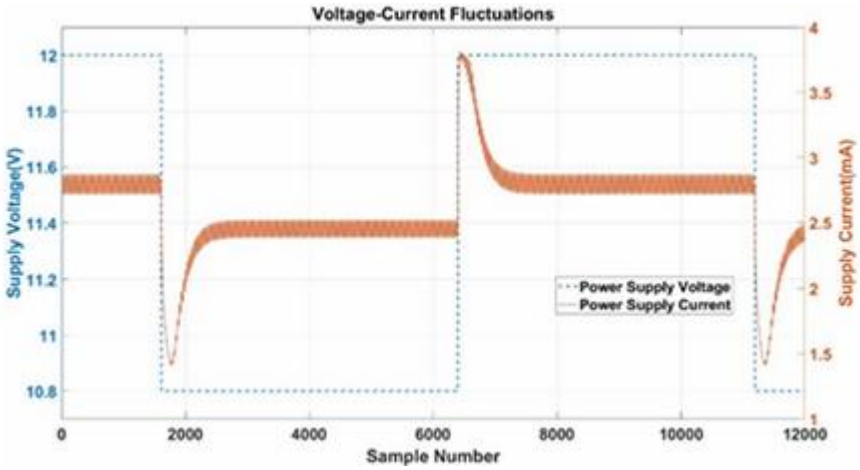

Figure 2. Voltage and Current Supply Waveforms

For the fundamental rms calculation, a slightly different mathematical formula is used. The formula for the true rms is given by equation (1). The supply current is comprised of two components, the DC and AC, which are denoted in equation (2).

$$I_{rms} = \sqrt{\frac{1}{T}\int_0^T I_{PS}(t)^2 dt} \qquad (1) \qquad \text{where } I_{ps}(t) = I_{DC} + I_{AC}(t) \qquad (2)$$

I_{DC} is the DC component and $I_{AC}(t)$ is a periodical and symmetrical around zero, time dependent function. By replacing the current, IPS(t) in equation (1) it takes the form,

$$I_{AC(rms)} = \sqrt{I_{rms}^2 - I_{DC}^2} \qquad (3)$$

From this point on, the value of $I_{AC(rms)}$ will be denoted as fundamental rms and it represents the AC component of the power supply current IPS. In Step 3, using the moving mean/rms technique, the mean and rms values for each step are calculated. The signal shown in Fig 2 is decomposed to the signals in Fig 3 with the use of equation (3) and moving mean and fundamental rms which represent the DC and the AC components of the Negative Step section of the IPS current.

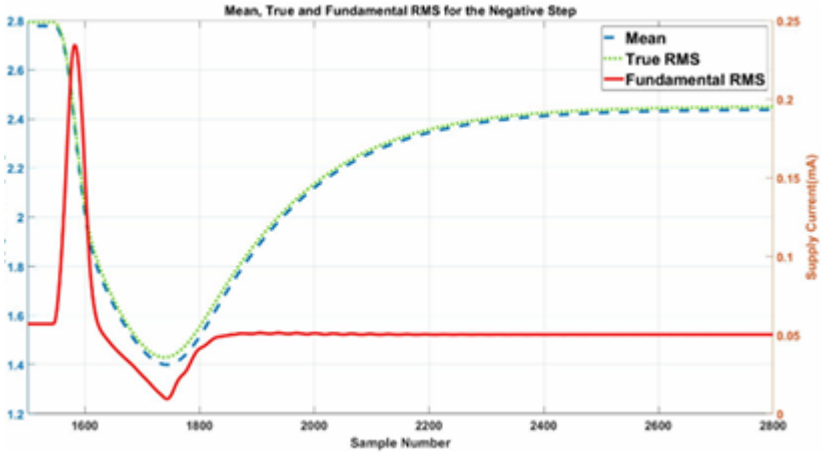

Figure 3. Mean, True and Fundamental RMS component of the Negative Step of the IPS current.

In Step 4, the values for the maximum overshooting and relaxation points along with the current/time pairs for each local point are calculated. To determine the current/time values of the relaxation point the angle of the slope of the signal is used. This angle is set to be 1o which is very close to stabilization line.

For the calculation of the damping point, a straight line is created which passes through both maximum and relaxation points. The gradient of the straight line is calculated. The damping point is defined to be the first point after the maximum overshooting point that has the same gradient value. The Points and the respected regions of interest are shown in Fig 4.

In Steps 5 and 6 the process of Steps 1 through 4 is repeated but for the transition of the power supply voltage from 90% to 100% of the nominal value (Positive Step), which produces similar signals.

The twelve current/time pairs from the mean, fundamental rms local maximum minimum, damping points and relaxation points for both positive and negative step are used to produce the signature in Step 7. The set of signatures that make up the training set are determined by the standard deviation created in Step 8 using the Monte Carlo simulations with a uniform distribution and a 10% value tolerance for every component of the circuit. A region where all measurements are thought to belong to a good/working CUT is created with the use of the standard deviation.

Repeating steps 1 through 7 while injecting errors into the CUT is the subsequent stage. For each CUT a fault introduced and a set of points will be extracted. Each new signature will be evaluated against the No-Fault signature by determining if the current/time pairs of the Faulty CUT signature are inside the detection area. At least one current/time pair needs to be outside the detection region for a faulty CUT to be detected. All twelve current/time pairs must be inside the detection area for the CUT to be classified as good. In all other cases, the CUT is classified as faulty. Hard faults (open and shorts) are inserted to the CUT to test the algorithm.

A short circuit to a specific component is indicated by placing a resistance of $R_p \leq 1\Omega$ in parallel to the corresponding component. To model an open circuit to component, the corresponding component is replaced by a resistance of value $R_p = 10M\Omega$ [10].

4 Experimental Results

The algorithm's overall detectability for the simulations was also employed to a Negative Feedback Amplifier and the results are shown in Table 1. The fundamental rms method managed to detect all injected faults of the CUT. For the experimental setup the algorithm is trained with 60 good circuits to obtain the points and regions of interest. Then the algorithm is tested with 100 CUTs for both test circuits, with a 50%/50% proportion for, Good/Faulty CUTs. The detection region varied from ±1σ to ±6σ. The result was that by decreasing the size of the detection region, the number of false negatives results (good CUTs being recognized as Faulty) increased and, vice-versa by increasing the size of the detection region the number of false positives (Faulty CUTs being recognized as good) increased.

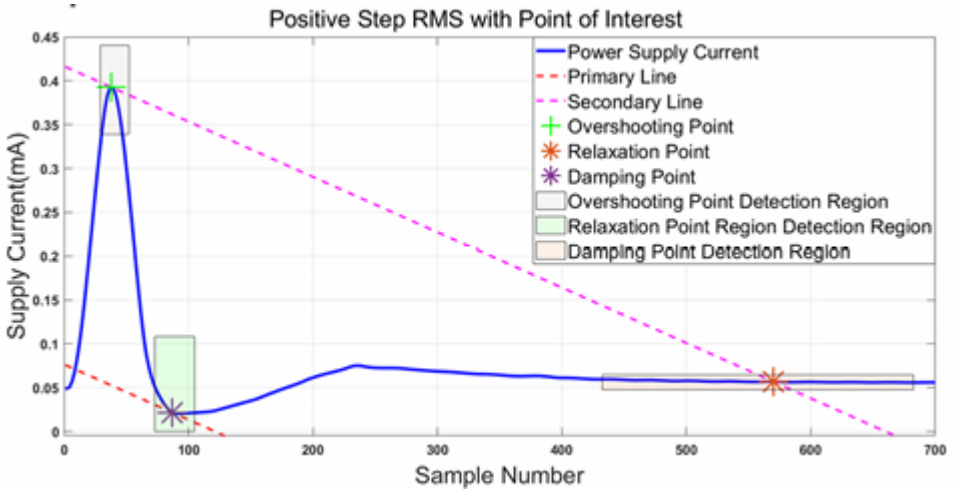

Figure 4. Positive Step with Points and regions of Interest.

Table II shows the detectability, in absolute numbers, of the algorithm in relation to the size of the detection region compared to the author's previous work [11]. It shows that a detection region with size of ±3σ around the mean value of the points of interest yields better detectability and accuracy.

Circuit	Number of Faults	Detected Faults without damping point	Detected Faults with damping point	Detectability(%) without damping point	Detectability(%) with damping point
Common Emitter Amplifier	22	22	22	100	100
Negative Feedback Amplifier	46	46	46	100	100

Table 1: Fault Detection results

Detection Range	True Positive without Damping Point	True Positive with Damping Point	True Negative without Damping Point	True Negative with Damping Point	False Positive without Damping Point	False Positive with Damping Point	False Negative without Damping Point	False Negative with Damping Point
±1σ	37	43	50	50	0	0	13	7
±2σ	41	48	50	50	0	0	9	2
±3σ	50	50	50	50	0	0	0	0
±4σ	50	50	44	49	6	1	0	0
±5σ	50	50	39	43	11	7	0	0
±6σ	50	50	32	38	18	12	0	0

Table 2: Fault Detectability for the Negative Feedback Amplifier

5 Conclusion

This paper presents an enhanced technique for detecting faults in analog circuits. This technique utilizes the fundamental RMS function, which can separate a signal into its basic DC and AC components.

The proposed technique calculates the overshooting/damping/stabilization values of the IPS of the CUT with respect to the time they occur. The algorithm applies the moving mean and moving rms algorithms to the IPS measurements to provide a signal that is smoother and can be analyzed in greater detail. Two circuits made use of the algorithm. A two-stage amplifier with negative feedback and a CE amplifier. 22 hard faults were introduced into the CE amplifier, and 46 hard faults were injected into the two-stage negative feedback amplifier. In comparison to the authors' previous work the algorithm was able to identify 100% of the faults on the CE amplifier and 100% of the injected faults for the negative feedback amplifier and reduced the number of false positives and false negatives in respect with the size of the detection range. The algorithm improved the previous detection range from ±3σ to ±2σ.

Based on the results, the next step is to improve the algorithm so that it can be applied to operational amplifier circuits in all of their operating modes, filters, amplifiers, and comparators. The algorithm at the time is refined so that it can operate both in unipolar and bipolar circuits.

6 References

[1] B.Olleta, H.Jiang, D.Chen, R.L.Geiger" Methods of testing analog and mixed signal using dynamic element matching for source linearization", US Patent Number:7.587.647B2, September 2009.

[2] Milne A, Taylor D, Naylor K, Assessing and comparing fault coverage when testing analogue circuits. In: Proceedings of IEEE conference on circuit devices and systems, vol. 144, 1; 1997. p. 1–4.

[3] R. Kondgunturi, E. Bradley, K. Maggard, C. Stroud "Benchmark circuits for analog and mixed signal testing.", Conference Proceedings - IEEE SOUTHEASTCON (1999) 1999-March 217 220

[4] A.A. Hatzopoulos, "Analog Circuit Testing", Proceedings of the 2017 IEEE 22nd International Mixed-Signals Test Workshop, IMSTW 2017.

[5] D. K. Papakostas, A.A. Hatzopoulos, "A Unified Procedure for Fault Detection of Analog and Mixed-Mode Circuits Using Magnitude and Phase Components of the Power Supply Current Spectrum", IEEE Transactions on instrumentation and measurement, vol. 57, No. 11, November 2008.

[6] A D. Spyronasios, M G. Dimopoulos, A. A. Hatzopoulos, “Wavelet Analysis for the Detection of Parametric and Catastrophic Faults in Mixed-Signal Circuits”, IEEE Transactions on instrumentation and measurement, vol. 60, No. 6, July 2011.

[7] M.F Toner, G.W. Roberts, “A BIST scheme for an SNR test of a sigma-delta ADC,” IEEE Int. Proc. Test. Conference 1993.

[8] C. T. Chen ,C. T. Yen, C. H. Wen, C. Y. Yang, C. H. Wu, K. C. Chern, M. Chen, Y. Y. Kuo, C. Y. Lee, J. N. Kao, S. Yi, “CNN-based Stochastic Regression for IDDQ Outlier Identification”, Proceedings of the IEEE VLSI Test Symposium, Vol: April 2020.

[9] K. Wang*, Y. Guana, D. Lib, X. Lic, J. Guand,“Research on Fault Diagnosis of Analog Circuit Based on Volterra Theory and Higher-Order Spectrum Analysis”, IOP Conf. Series: Materials Science and Engineering 782 (2020) 032096.

[10] P. Kabisatpathy, A. Barua, S. Sinha, ”Fault Diagnosis of Analog Integrated Circuits”, 1st ed., Springer, 2005, pp 30-31.

[11] V. Vassios, A. Hatzopoulos, D. Papakostas,” Improved Fault Detection of Analog Circuits by utilizing the Fundamental RMS of the Supply Current Fluctuation”,12th International Conference on Modern Circuits and Systems Technologies (MOCAST23), University of West Athens, Athens, pp. 28-30, June 2023